Microporous and Mesoporous Materials 116 (2008) 171–179

Contents lists available at ScienceDirect

Microporous and Mesoporous Materials

journal homepage: www.elsevier.com/locate/micromeso

Synthetic design towards targeted chiral anionic surfactant templated chiral mesoporous silica

Haiying Jin, Huibin Qiu, Chuanbo Gao, Shunai Che *

School of Chemistry and Chemical Technology, State Key Laboratory of Composite Materials, Shanghai Jiao Tong University, 800 Dongchuan Road, Shanghai 200240, PR China

ARTICLE INFO

Article history:
Received 11 February 2008
Received in revised form 28 March 2008
Accepted 31 March 2008
Available online 16 April 2008

Keywords:
Chiral
Mesoporous silica
Pitch length
Self-assembly
2D-hexagonal

ABSTRACT

Chiral mesoporous silica (CMS) with highly ordered helical nano-sized channels was synthesized by using chiral anionic amphiphilic molecules (*N*-acyl-L-alanine) as template upon a co-structural-directing-agent (CSDA) method. Synthetic conditions, such as ionization degree of the surfactant, CSDA/surfactant molar ratio, reaction temperature, the carbon chain length, and the type of base that affect the mesostructure and morphology of the CMSs have been extensively studied. It was found that: (i) in the synthesis-space diagram of mesophases, the CMS mesostrucrue locates within the area of two dimensional (2D) hexagonal which is a neighbor of lamellar and bicontinuous $Ia\bar{3}d$ mesostructures; (ii) the generation of CMS demands very rigorous micellar curvature which was mainly controlled by the ionization degree of the surfactant controlled by acid addition amount, CSDA/surfactant molar ratio and the carbon chain length; (iii) the CMS can be synthesized in a wide reaction temperature range of 25–100 °C; and (iv) the pore diameter of the CMS was decreased with decreasing size of the counterion.

© 2008 Elsevier Inc. All rights reserved.

1. Introduction

Helical architecture is one of the most fascinating structures in nature which is common on both microscopic and macroscopic levels. So far, various supramolecular helical entities have been formed by different kinds of small molecules through the self-assembling process [1,2]. The chiral self-assembly of amphiphilic molecules is of particular interest as a fundamental synthetic strategy in nature [3–9]. On the other hand, helical inorganic superstructures have also been created by using the organic template approach accompanied with the sol–gel process [10–12]. These materials are of great potential application in the fields of chiral selectivity, chiral recognition, and chiral catalysis.

Recently, we have achieved the first synthesis of chiral mesoporous silica (CMS) with highly ordered helical nano-sized channels through the self-assembling of chiral anionic amphiphiles based upon a co-structure-directing-agent (CSDA) method [13]. It was found that the crystal morphology of CMS greatly depends on the stirring rate in the initial stage of the synthesis [14]. Importantly, the enantiopurity of CMS can be controlled by the reaction temperature and the stereochemistry of the chiral amphiphilic molecule [15]. Besides, racemic CMSs were successfully obtained by using several achiral cationic and anionic amphiphilic molecules as templates [15–21]. A phase transition from 2D-rectangular *p2gg* to 2D-hexagonal *p6mm* has been found in the CMS synthesis by adjusting the basicity of the reaction mixture [22]. However, due to the complication of CMS synthesis, the above understanding is still far less to reveal the formation mechanism of CMS.

Herein, we concentrate our efforts on the effects of the detail synthetic parameters on the mesostructure and morphology of CMS. Chiral anionic amphiphilic molecules *N*-acyl-L-alanine (C_n-L-Ala, n = 12, 14, and 16) were selected as template due to their feature to form uniform CMS crystals. In a typical synthesis, the chiral anionic amphiphilic molecule was neutralized with hydroxide and then partially acidified with mineral acid. *N*-trimethoxysilylpropyl-*N*,*N*,*N*-trimethylammonium chloride (TMAPS) was chosen as CSDA since it has a constant positive charge. In this work, the dominating synthesis parameters, including the ionization degree of surfactant, TMAPS/surfactant molar ratio, reaction temperature, the carbon chain length, and the type of couterions were carefully adjusted to reveal their effects upon the morphology and microstructures of CMS. The present study provides a comprehensive study on the synthetic control of CMS.

2. Experimental section

2.1. Chemicals

Chiral anionic amphiphilic molecules (C_n-L-Ala, n = 12, 14, and 16) were synthesized according to the previous reports [23]. Tetraethoxylsilane (TEOS) was purchased from TCI and TMAPS (50% in methanol) from Azmax. All chemicals were used as received without further purification.

* Corresponding author. Tel.: +86 21 54742852.
E-mail address: chesa@sjtu.edu.cn (S. Che).

1387-1811/$ - see front matter © 2008 Elsevier Inc. All rights reserved.
doi:10.1016/j.micromeso.2008.03.035

2.2. Synthesis

In a typical synthesis, C_{16}-L-Ala (0.327 g, 1 mmol) and 0.1 M NaOH (10.0 g, 1 mmol) was dissolved in deionized water (22.7 g) with stirring at room temperature. 0.1 M HCl (1.4 g, 0.14 mmol) was then added to the above solution under vigorous stirring at room temperature to partially acidify the salt. After the mixture was stirred for 1 h, a mixture of TEOS (1.40 g, 6.72 mmol) and TMAPS (0.20 g, 0.39 mmol) was added to the mixture with stirring at room temperature for 10 min followed by statical placement for 2 h. The molar composition ratio of the gel obtained was C_{16}-L-Ala:NaOH:TEOS:TMAPS = 1:0.86:6.72:0.39. The mixture was finally cured at 80 °C for additional 15 h. The solid product was recovered by centrifugal separation and dried at 80 °C. Both of the anionic surfactants and the organics of the CSDA used were removed by calcination at 550 °C for 6 h.

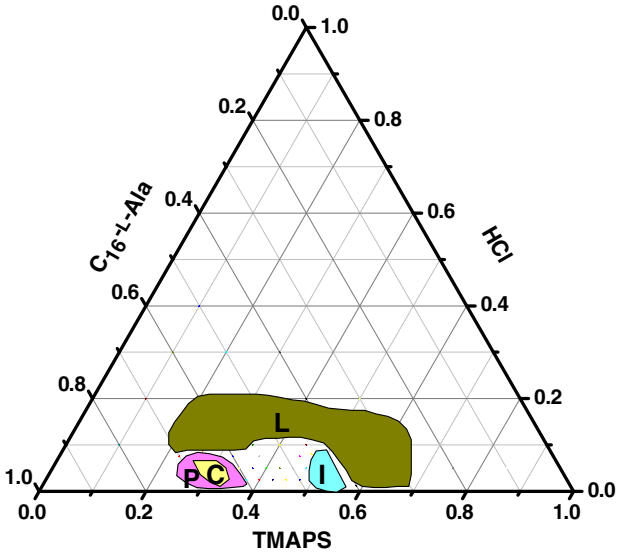

Fig. 1. Synthesis-space diagram of C_{16}-L-Ala template mesoporous silicas. Each mixture had a constant H_2O/C_{16}-L-Ala molar ratio of 1722 and TEOS/C_{16}-L-Ala molar ratio of 7. All the mesoporous silicas were synthesized under static condition at 80 °C for 1 day. L: lamellar, I: bicontinous *Ia*$\bar{3}$*d*, P: 2D-hexagonal *p6mm* and C: CMS phase.

2.3. Characterization

Powder XRD patterns were recorded on a Rigaku X-ray diffractometer D/MAX-2200/PC equipped with Cu Kα radiation (40 kV, 20 mA). HRTEM was performed with a JEOL JEM-3010 microscope operating at 300 kV (Cs = 0.6 mm, resolution 1.7 nm). The microscopic features of the sample were observed with SEM (JEOL JSM-7401F). The nitrogen adsorption–desorption isotherms were obtained at −196 °C on a Quantachrome NOVA 4200E surface area and pore size analyzer.

3. Results and discussion

It was previously demonstrated that in the synthesis of CMS, the positively charged ammonium site of TMAPS interacts electrostatically with the negatively charged head group of the C_n-L-Ala while the alkoxysilane site co-condenses with TEOS [13]. The degree of ionization of the surfactant can be readily changed by additional base or acid, which results in different micellar charge density and thus different mesostructures [24]. Fig. 1 shows the ternary phase diagrams of C_{16}-L-Ala, TMAPS and HCl in which 60 experiments were performed. It can be seen that the mesostructure and morphology of the resultant mesoporous silica greatly depend on the proportion of acid and CSDA as reported previously [24]. Mesoporous silicas with lamellar, bicontinuous *Ia*$\bar{3}$*d*, and 2D-hexagonal *p6mm* mesostructures, with increasing micellar curvature [24], were obtained separately in a wide range of composition. The mesostructure of CMS was found to be located in the area of 2D-hexagonal indicating that it may be a special phase of 2D-hexagonal self-assembled by propeller-like rod micelles as reported previously [15].

3.1. Effect of acid/surfactant molar ratio on the mesostructure and morphology of CMS

To investigate the effect of acid component on the mesostructure and morphology of CMS, the HCl/C_{16}-L-Ala molar ratio was adjusted with the synthesis molar composition: 1.0C_{16}-L-Ala/1.0NaOH/0.45TMAPS/*x*HCl/7.0TEOS/1680.0H_2O. It was found that CMS with uniform twisted hexagonal rod-like morphology can only be fabricated in a narrow range of HCl/C_{16}-L-Ala molar ratio (x = 0.06–0.12) (Fig. 2b1, c1 and d1). The average outer diameters of twisted hexagonal rod-like morphology (with hexagonal) were

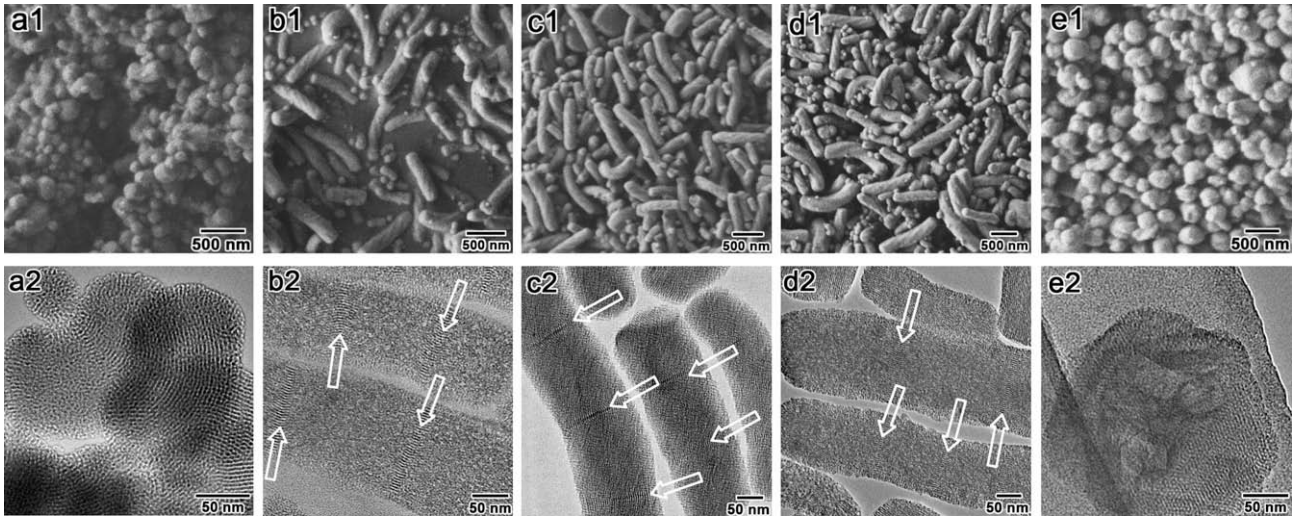

Fig. 2. SEM and TEM images of the CMSs synthesized with various HCl/C_{16}-L-Ala molar ratio. The molar composition of the reaction mixture was C_{16}-L-Ala:NaOH:HCl:TMAPS:TEOS:H_2O = 1:1:*x*:0.43:7:1722, x = 0.04 (a), 0.06 (b), 0.08 (c), 0.12 (d) and 0.16 (e).

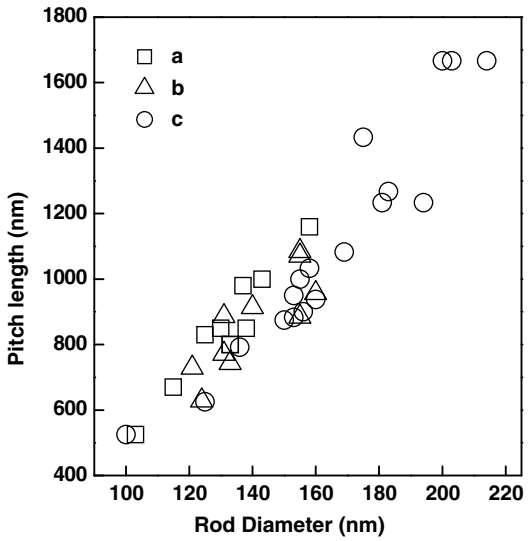

Fig. 3. Pitch length to rod diameter dependence of the samples synthesized with $x = 0.06$ (a), 0.08 (b) and 0.12 (c).

increased from ~133 and ~141 to ~165 nm with increasing molar ratio of HCl/C_{16}-L-Ala from 0.06 to 0.08 and 0.12. The mesoporous silica particles lost regular crystalline morphology when the HCl/C_{16}-L-Ala molar ratio was further decreased ($x < 0.06$) or increased ($x > 0.12$). This indicated that the generation of CMS demands very rigorous ionization degree of the chiral amphiphilic molecule, which controls the molecular packing to form helical propeller-like micelle as we reported previously [15,24].

HRTEM images (Fig. 2b2, c2 and d2) revealed the ordered fringes in a distance as indicated by the arrows, indicating that all of these samples possess highly ordered 2D-hexagonal chiral channels running inside winding around the central axis of the rod as reported in our previous work [13]. As shown in Fig. 3, the pitch length increases linearly with increasing the rod diameter, with a constant ratio of pitch length/rod diameter in any case of HCl/C_{16}-L-Ala molar ratio.

The XRD patterns (Fig. 4 left) of the calcined samples showed three well-resolved 10, 11 and 20 reflections of the 2D-hexagonal *p6mm* in the range of $2\theta = 1.5°$–$6.0°$, indicating that these samples have highly ordered 2D-hexagonal mesostructure. The nitrogen

Table 1
The properties of mesoporous silicas synthesized with various HCl/C_{16}-L-AlaS molar ratios

HCl/C_{16}-L-AlaS molar ratio	BET surface (m^2/g)	Pore diameter (nm)	Pore volume (mm^3/g)
0.06	322	2.7	340
0.08	776	2.7	600
0.12	697	3.4	520

adsorption–desorption curves (Fig. 4 right) of these samples show a type IV feature with a capillary condensation step at ~0.4 in relative pressure, which confirmed the existence of uniform mesopores. The BET surface areas and pore volumes were in the range of 322–697 m^2/g and 340–600 mm^3/g, respectively. The pore diameters were 2.7, 2.7 and 3.4 nm for sample synthesized with $x = 0.06$, 0.08 and 0.12, respectively (Table 1). The decrease of acid/surfactant molar ratio increased the ionization degree of the anionic amphiphilic molecules and thus increased its electrostatic interaction with the quaternary ammonium group of CSDA. The strong interaction between the surfactant head group and quaternary ammonium group of CSDA will drive the wall into the core of the micelle.

3.2. Effect of CSDA/surfactant molar ratio on the mesostructure and morphology of CMS

To observe the effect of CSDA/surfactant molar ratio on the mesostructure and morphology of CMS, the TMAPS/C_{16}-L-Ala molar ratio was adjusted in the range of 0.1–1.5 with the synthesis molar composition: 1.0C_{16}-L-Ala/1.0NaOH/yTMAPS/0.1HCl/7.0TEOS/1680.0H_2O. As shown in Fig. 5, uniform CMS crystals can be obtained when the TMAPS/C_{16}-L-Ala molar ratio is in the range of 0.4–0.6. Both the diameter and length of the rods maintain similar with varying the TMAPS/C_{16}-L-Ala molar ratio, which are 130–180 nm and 1–6 μm, respectively. The highly ordered 2D-hexagonal chiral channels of these CMSs were confirmed by the TEM images as shown in Fig. 5b2, c2, d2 and e2. It can be seen that the formation of CMS is strictly dominated by the CSDA/surfactant molar ratio. The TMAPS/C_{16}-L-Ala molar ratio applied in the CMS formation is around 0.5 indicating that a quaternary ammonium group of TMAPS interacts averagely with two carbonate groups of C_{16}-L-Ala, as to afford a proper micellar curvature for the generation of helical propeller-like micelle [15,24].

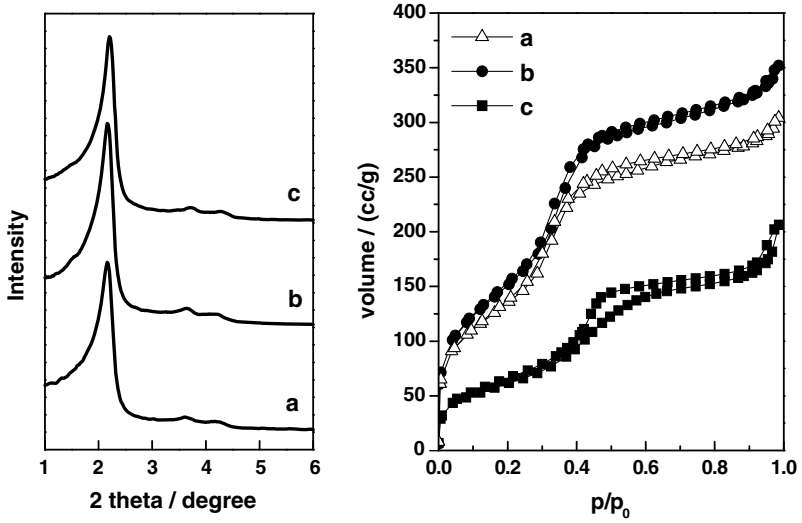

Fig. 4. XRD patterns (left) and N_2 adsorption–desorption isotherms (right) of the calcined CMSs synthesized with $x = 0.06$ (a), 0.08 (b) and 0.12 (c).

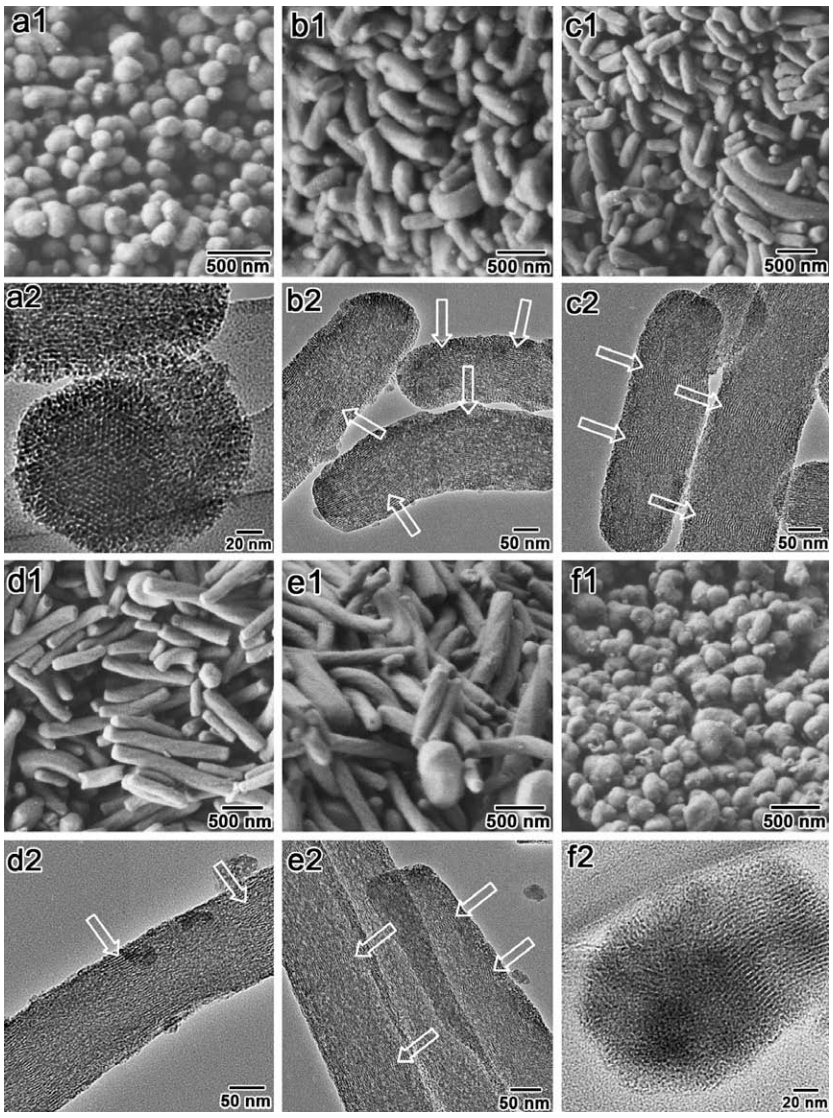

Fig. 5. SEM and TEM images of the calcined CMSs synthesized with various TMAPS/C_{16}-L-Ala molar ratio. The molar composition of the reaction mixture was C_{16}-L-Ala:NaOH:HCl:TMAPS:TEOS:H_2O = 1:1:0.1:*y*:7:1722, *y* = 0.30 (a), 0.40 (b), 0.45 (c), 0.53 (d), 0.60 (e) and 0.70 (f).

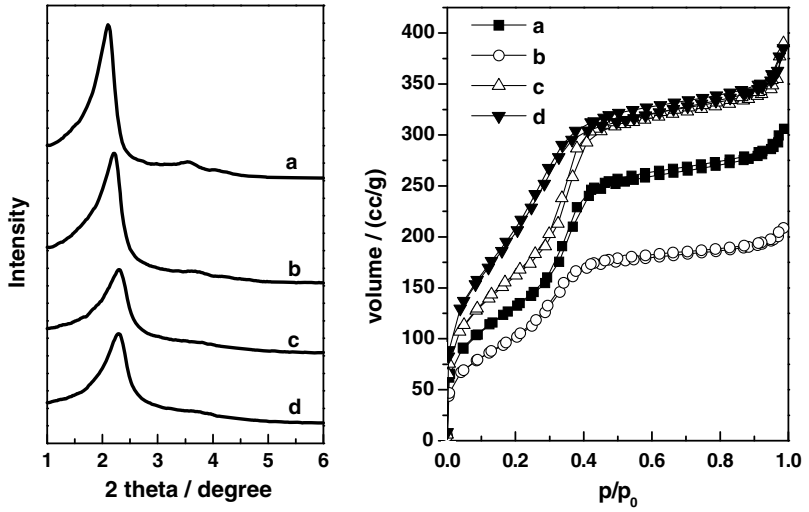

Fig. 6. XRD patterns (left) and N_2 adsorption–desorption isotherms (right) of the calcined CMSs shown in Fig. 5. (a) *y* = 0.40, (b) *y* = 0.45, (c) *y* = 0.53 and (d) *y* = 0.60.

Table 2
The properties of mesoporous silicas synthesized with various TMAPS/C_{16}-L-AlaS molar ratios

TMAPS/C_{16}-L-AlaS	BET surface (m^2/g)	Pore diameter(nm)	Pore volume (mm^3/g)
0.40	680	2.9	530
0.45	510	2.7	360
0.50	992	2.5	660
0.60	760	2.5	490

XRD patterns of the CMSs (Fig. 6 left) show that these samples possess highly ordered 2D-hexagonal *p6mm* mesostructure. The peaks of 10, 11 and 20 moved to low angle with increasing the TMAPS/C_{16}-L-Ala molar ratio, indicating an increase of the *d*-spacing of the mesostructure. The nitrogen adsorption–desorption curves (Fig. 6 right) of these samples show a type IV feature with a capillary condensation step at ~0.4 in relative pressure. The BET surface areas and pore volumes were 992–510 m^2/g and 360–660 mm^3/g, respectively. The pore diameters are 2.9, 2.7, 2.5 and 2.5 nm for sample synthesized with y = 0.40, 0.45, 0.53 and 0.60, respectively (Table 2). It indicated that the increase of CSDA/surfactant molar ratio enhanced the electrostatic interaction between the micelle and the quaternary ammonium group of CSDA wall and thus decreased the distance of them which made a smaller pore size.

3.3. Effect of temperature on the mesostructure and morphology of CMS

The temperature of the reaction system is an important factor in the determination of the mesostructure by controlling the thermodynamic and kinetics of both the packing of the amphiphilic molecules and the condensation of the silica precursor. Herein, different reaction temperatures in the range of 25–80 °C were applied to form mesoporous silicas. The synthesis molar composition was: 1.0C_{16}-L-Ala/1.0NaOH/0.45TMAPS/0.1HCl/7.0TEOS/1680.0H_2O. It was found that the materials were composed of uniform open-ended tubes with outer diameter of 100–200 nm and length of 1–5 μm (Fig. 7a1) under the reaction temperature of 25 °C. TEM image

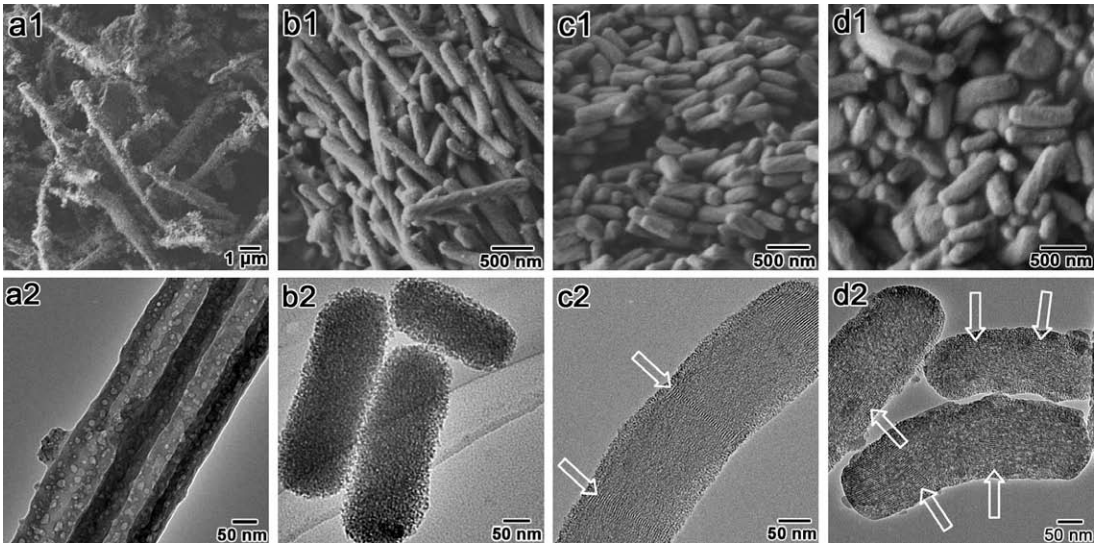

Fig. 7. SEM and TEM images of the calcined mesoporous silicas synthesized at different reaction temperatures of 25 (a), 40 (b), 60 (c) and 80 °C (d).

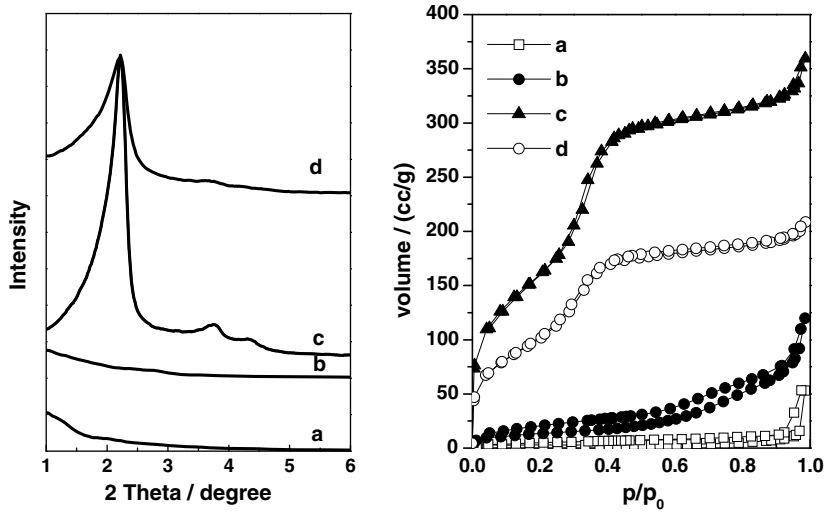

Fig. 8. XRD patterns (left) and N_2 adsorption–desorption isotherms (right) of the calcined mesoporous silicas shown in Fig. 7.

(Fig. 7a2) showed that the tube wall was composed of disordered nanoscaled channels which are much larger than those in the CMSs.

With increasing the reaction temperature to 40 °C, mesoporous silica crystals with uniform twisted rod-like morphology can be obtained (Fig. 7b1). However, as shown by the TEM image (Fig. 7b2), the highly ordered twisted mesopores are absent in such material. The crystal recovered its helical mesostructure when the reaction temperature was increased to 60 °C and 80 °C (Fig. 7c1, c2, d1, d2). The lengths and diameters of the CMSs were 0.5–2.0 μm and 100–200 nm, respectively. On the other hand, the product showed irregular morphology when the temperature was further enhanced to 100 °C, which may be induced by the disorganized packing of the amphiphilic molecules.

Table 3
The properties of mesoporous silicas synthesized at different reaction temperatures

Reaction temperature (°C)	BET surface (m^2/g)	Pore diameter (nm)	Pore volume (mm^3/g)
60	806	2.7	610
80	510	2.7	360

As shown in Fig. 8 (left) a and b, no resolved peaks was observed from the XRD patterns for the samples synthesized at 25 and 40 °C, largely because of the presence of the disordered mesostructures. The N_2 adsorption–desorption isotherms (Fig. 8 (right) a and b) of the two calcined samples exhibit very low sorption in the mesoscale, indicating the low quality of the mesoporous system. However, the samples obtained at 60 and 80 °C showed highly ordered 2D-hexagonal *p6mm* mesostructure (Fig. 8 (left) c and d) and high BET surface area (806 and 511 m^2/g) and pore volume (610 and 360 mm^3/g), with the same pore diameter of 2.7 nm (Table 3).

3.4. Effect of carbon chain length of the template on the mesostructure and morphology of CMS

C_{12}-L-Ala and C_{14}-L-Ala, with shorter carbon chain length, were also applied to prepare mesoporous silica materials. The products synthesized with C_{12}-L-Ala are irregular in morphology (Fig. 9a1)

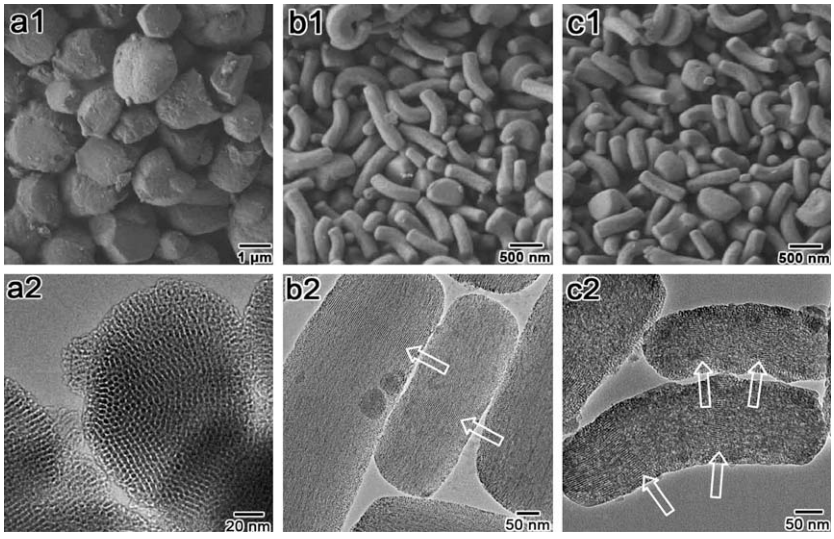

Fig. 9. SEM and TEM images of the calcined mesoporous silicas synthesized with different surfactant of C_{12}-L-Ala (a), C_{14}-L-Ala (b) and C_{16}-L-Ala (c) as templates.

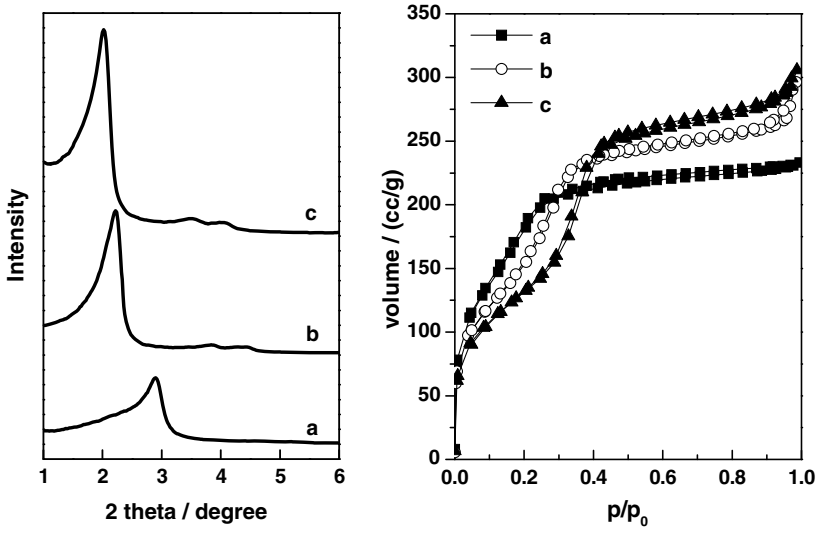

Fig. 10. XRD patterns (left) and N_2 adsorption–desorption isotherms (right) of the calcined mesoporous silicas shown in Fig. 9.

while C_{14}-L-Ala and C_{16}-L-Ala can afford uniform CMS crystals as shown in Fig. 9b1, b2, c1 and c2. However, it was found that CMS could be formed in a wider range of reaction composition with C_{16}-L-Ala as template than that with C_{14}-L-Ala as template. Thus C_n-L-Ala with carbon chain length of 16 is most favorable for the formation of CMS. It is known that the micellar curvature decreases with increasing carbon chain length due to the increase of micelle diameter. Lower micellar curvature in the 2D-hexagonal region may favor the generation of CMS [22].

Table 4
The properties of mesoporous silicas synthesized with different surfactants having different chain length

Surfactant	BET surface (m^2/g)	Pore diameter (nm)	Pore volume (mm^3/g)
C_{12}-L-AlaS	780	2.0	390
C_{14}-L-AlaS	764	2.5	510
C_{16}-L-AlaS	680	2.9	530

XRD pattern of the sample synthesized with C_{12}-L-Ala showed only one broad peak in the range of $2\theta = 1.0°–6.0°$ (Fig. 10 left a) which may be due to its disordered mesostructure (Fig. 9a2). However, the samples synthesized with C_{14}-L-Ala and C_{16}-L-Ala showed highly ordered 2D-hexagonal *p6mm* symmetry (Fig. 10 left b and c). Besides, it was found that the 10 peak moved to smaller angle with increasing the carbon chain length. The nitrogen adsorption–desorption curves (Fig. 10 right) showed a type IV feature and the pore diameters were 2.0, 2.5 and 2.9 nm (Table 4) for sample synthesized with C_{12}-L-Ala, C_{14}-L-Ala and C_{16}-L-Ala, respectively, which was consistent with our conclusion that the micelle diameter increases with increasing the carbon chain length.

3.5. Effect of counterion type on the mesostructure and morphology of CMSs

The formation of mesostructure can be affected by the counteranions in terms of the adsorption strength on the headgroups of the surfactant micelle [25]. To investigate the effect of different

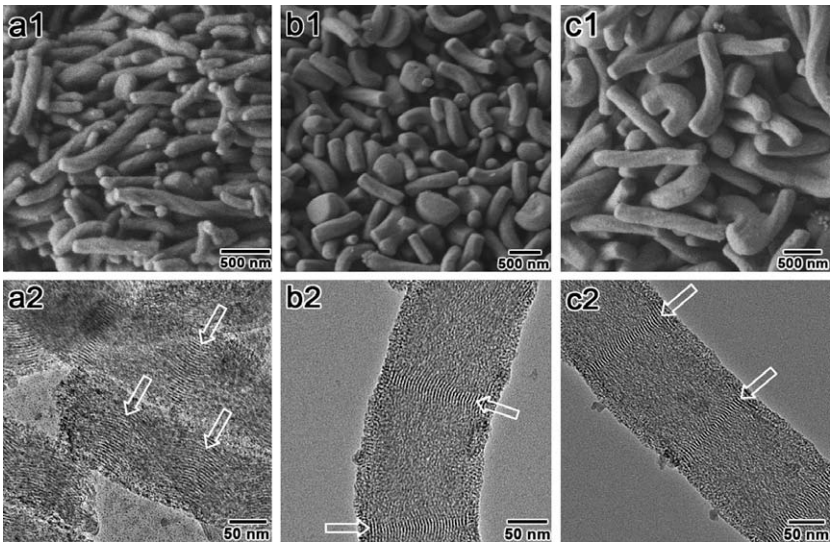

Fig. 11. SEM and TEM images of the calcined CMSs synthesized with different bases of LiOH (a), NaOH (b) and KOH (c).

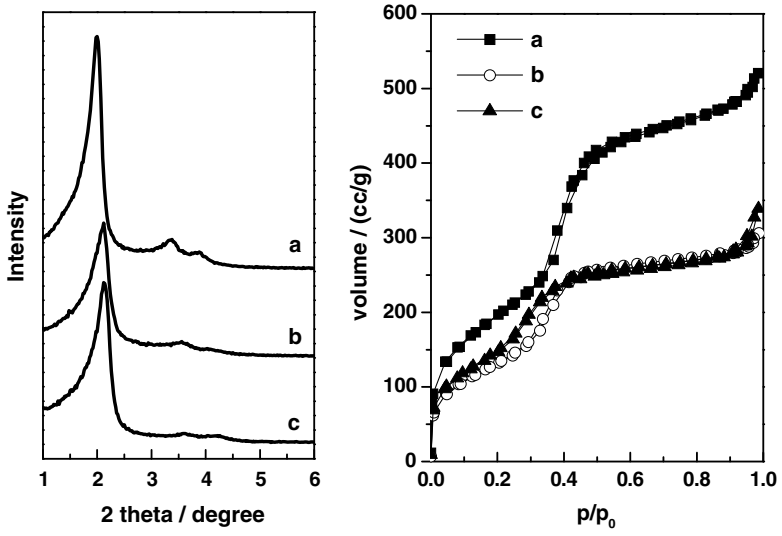

Fig. 12. XRD patterns (left) and N_2 adsorption–desorption isotherms (right) of the calcined CMSs shown in Fig. 11.

Table 5
The properties of mesoporous silicas synthesized with different bases

Base	BET surface (m^2/g)	Pore diameter (nm)	Pore volume (mm^3/g)
LiOH	671	3.2	600
NaOH	680	2.9	530
KOH	731	2.5	570

counter cations in the reaction system on the formation of CMS, LiOH, NaOH and KOH were used to ionize the anionic amphiphilic molecules. SEM images (Fig. 11a1, b1 and c1) revealed that all of the samples were composed of the twisted hexagonal rod-like particles with length of 0.5–1.0 μm and diameter of 50–150 nm. TEM images (Fig. 11a2, b2 and c2) revealed the highly ordered twisted mesochannels, typically for CMS.

Three well-resolved peaks could be found in the range of $2\theta = 1°–6°$, indexed as 10, 11 and 20 reflections, based on the 2D-hexagonal *p6mm*, indicating that these materials had highly ordered hexagonal mesostructures (Fig. 12 left). It can be seen that the 10 peak moved to larger angle with changing the base from LiOH, NaOH to KOH. Nitrogen adsorption–desorption isotherms of the calcined samples (Fig. 12 right) showed a type IV feature, indicating the existence of uniform mesopores. The pore diameters were 3.2, 2.9 and 2.5 nm for the sample synthesized with LiOH, NaOH and KOH, respectively (Table 5). As discussed above, a quaternary ammonium group of TMAPS interacts averagely with two carbonate groups of C_{16}-L-Ala. It means that there must be one counter ion occupied by one of the two carbonate groups of C_{16}-L-Ala. It was reported that K^+, Na^+ and Li^+ were hydrated in the solution and the hydrated ionic radii decreased in the following order: $Li^+ > Na^+ > K^+$. The effect of the counter ionic radii on the pore size of the CMS can be understood by considering the micelle size hydrophobic tails and hydrophilic head groups. Ions with smaller ionic radii bind more closely and strongly on the headgroup of the surfactant [25]. Thus, the micellar curvature decreases with decreasing the ionic radii and results in an increase of micelle diameter as reported previously [24]. However, since the micellar surface and the silica wall surface are both negatively charged, it can be considered that the decrease of the ionic radii of the cationic ions will enhance their electrostatic force to make the two surfaces closer and thus decrease the micelle diameter. Herein, the pore diameter decreased with increasing of ionic radii, indicating that the latter seems predominant over the former.

The handedness of these CMSs was estimated by counting characteristic morphologies from 500 randomly chosen crystals in the SEM images, and the maximum left-/right-handed ratios proved to be 6.5/3.5, which is the same with our previous work [13].

3.6. Mesostructure and morphology transformation with reaction time

The structural and morphologic evolution of the CMS can be well understood by investigating the formation process. Herein, the reaction process of a synthesis mixture with molar composition of $1.0C_{16}$-L-Ala/1.0NaOH/0.45TMAPS/0.1HCl/7.0TEOS/$1680.0H_2O$ was studied. Typically, the mixture was stirred for 10 min at 25 °C and then allowed to react under static conditions at 80 °C and sampled at different reaction time between 0.5 h and 1 day.

As shown in Fig. 13a, the material sampled at 0.5 h revealed rod-like aggregates containing monolith morphology. Straight rod-like crystals with rough surface were formed after 50 min (Fig. 13b). With increasing reaction time to 2.5 h and 1 day the straight rod finally showed helical curves as typically for CMS (Fig. 13c and d). As shown by the XRD patterns (Fig. 14), the 10, 11 and 20 peaks of these samples grew up with increasing reaction time. It indicated that (i) at the initial stage, the mesostructure of the CMS is not very ordered; (ii) the material is somewhat soft and is under a structural transformation; (iii) the CMS mesostructure grew up together with the crystalline morphology and finally became highly ordered.

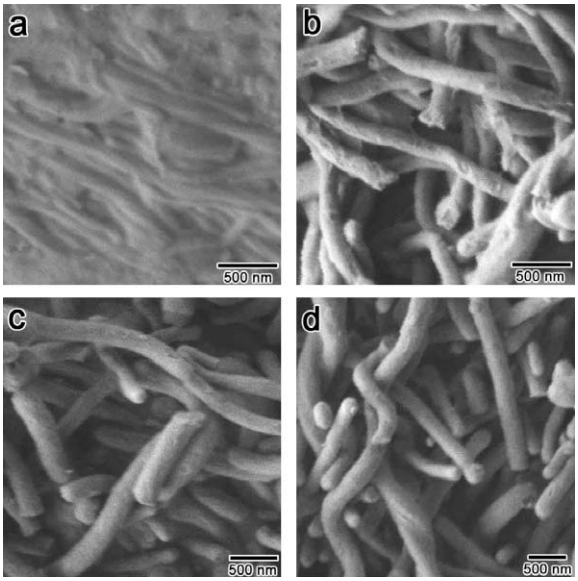

Fig. 13. SEM images of the CMSs synthesized at 80 °C with different reaction time of 30 min (a), 50 min (b), 2.5 h (c) and 1 day (d).

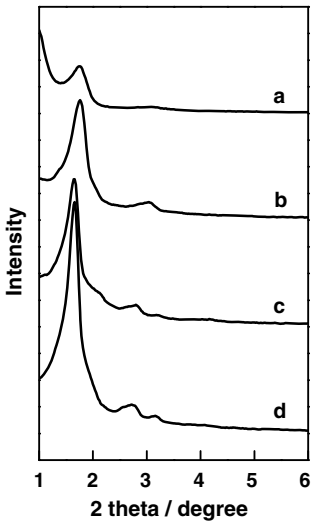

Fig. 14. XRD patterns of the CMSs shown in Fig. 13.

4. Conclusions

In conclusion, a systematic study was carried out for C_n-L-Ala based CMS synthesis. The effects of different synthetic parameters on the mesostructure and morphology of the CMSs were investigated in detail. The morphology and microstructures of CMS have been controlled by the ionization degree of surfactant and TMAPS/surfactant molar ratio. It has been found that highly ordered CMS has been obtained at wide reaction temperature range of 25–100 °C; the surfactant with carbon chain length of 14 and 16 is most suitable for the formation of the twisted rod-like morphology. We hope the present study could make contributions to a fur-

ther understanding of the CMS formation and help us to precisely control the property of the CMS materials.

Acknowledgments

This work was supported by the National Natural Science Foundation of China (Grant No. 20425102 and 20521140450) and the China Ministry of Education.

Appendix A. Supplementary data

Supplementary data associated with this article can be found, in the online version, at doi:10.1016/j.micromeso.2008.03.035.

References

[1] A.R.A. Palmans, E.W. Meijer, Angew. Chem. Int. Ed. 46 (2007) 8948.
[2] D.B. Amabilino, J. Veciana, Top. Curr. Chem. 265 (2006) 253.
[3] T. Kunitake, Y. Okahata, M. Shimomura, S. Yasunmi, K. Takarabe, J. Am. Chem. Soc. 103 (1981) 5401.
[4] N. Nakashima, S. Asakuma, T. Kunitake, J. Am. Chem. Soc. 107 (1985) 509.
[5] J.-H. Fuhrhop, P. Schnieder, E. Boekema, W. Helfrich, J. Am. Chem. Soc. 110 (1988) 2861.
[6] D.A. Frankel, D.F. O'Brien, J. Am. Chem. Soc. 116 (1994) 10057.
[7] T. Imae, Y. Takahashi, H. Muramatsu, J. Am. Chem. Soc. 114 (1992) 3414.
[8] B.N. Thomas, C.M. Lindemann, R.C. Corcoran, C.L. Contant, J.E. Kirsch, J.P. Persichini, J. Am. Chem. Soc. 124 (2002) 1227.
[9] J.H. Jung, Y. Do, Y-A. Lee, T. Shimizu, Chem. Eur. J. 11 (2005) 5538.
[10] J.H. Jung, Y. Ono, K. Hanabusa, S. Shinkai, J. Am. Chem. Soc. 122 (2000) 5008.
[11] Y. Yang, M. Suzuki, S. Owa, H. Shirai, K. Hanabusa, Chem. Commun. (2005) 4462.
[12] A.M. Seddon, H.M. Patel, S.L. Burkett, S. Mann, Angew. Chem. Int. Ed. 41 (2002) 2988.
[13] S. Che, Z. Liu, T. Ohsuna, K. Sakamoto, O. Terasaki, T. Tatsumi, Nature 429 (2004) 281.
[14] H. Jin, Z. Liu, T. Ohsuna, O. Terasaki, Y. Inoue, K. Sakamoto, T. Nakanishi, K. Ariga, S. Che, Adv. Mater. 18 (2006) 593.
[15] H. Qiu, S. Wang, W. Zhang, K. Sakamoto, O. Terasaki, Y. Inoue, S. Che, J. Phys. Chem. C 112 (2008) 1871.
[16] X. Wu, H. Jin, Z. Liu, T. Ohsuna, O. Terasaki, K. Sakamoto, S. Che, Chem. Mater. 18 (2006) 241.
[17] X. Wu, J. Ruan, T. Ohsuna, O. Terasaki, S. Che, Chem. Mater. 19 (2007) 1577.
[18] B.G. Trewyn, C.M. Whitman, V.S.-Y. Lin, Nano Lett. 4 (2004) 2139.
[19] B. Wang, C. Chi, W. Shan, Y. Zhang, N. Ren, W. Yang, Y. Tang, Angew. Chem. Int. Ed. 45 (2006) 2088.
[20] Q. Zhang, F. Lü, C. Li, Y. Wang, H. Wan, Chem. Lett. 35 (2006) 190.
[21] S. Yang, L. Zhao, C. Yu, X. Zhou, J. Tang, P. Yuan, D. Chen, D. Zhao, J. Am. Chem. Soc. 128 (2006) 10460.
[22] H. Qiu, Y. Sakamoto, O. Terasaki, S. Che, Adv. Mater. 20 (2008) 425.
[23] M. Takehara, I. Yoshimura, K. Takizawa, R. Yoshida, J. Am. Oil Chem. Soc. 49 (1972) 157.
[24] C. Gao, H. Qiu, W. Zeng, Y. Sakamoto, O. Terasaki, K. Sakamoto, Q. Chen, S. Che, Chem. Mater. 18 (2006) 3904.
[25] S. Che, S. Lim, M. Kaneda, H. Yoshitake, O. Terasaki, T. Tatsumi, J. Am. Chem. Soc. 124 (2002) 13962.